Coupling of the Guanosine Glycosidic Bond Conformation and the Ribonucleotide Cleavage Reaction: Implications for Barnase Catalysis

Short Title: GpA hydrolysis mechanism

Key words: Potential of mean force calculations; dinucleotides; conformational analysis; RNA-protein interactions; nucleophilic attack

The work was performed at Departament de Química Física i Analítica, Universitat Jaume I, 12071 Castelló, Spain

Maite Roca,[1] Leonardo De Maria,[2] Shoshana J. Wodak,[3,4] Vicente Moliner,[1] Iñaki Tuñón,[5] and Jesús Giraldo[6*]

[1] Departament de Química Física i Analítica, Universitat Jaume I, 12071 Castelló, Spain
[2] Novozymes A/S, 2880 Bagsvaerd, Denmark
[3] Hospital for Sick Children, 555 University Ave, Toronto M5G 1X8, Canada
[4] Departments of Biochemistry and Medical Genetics, University of Toronto, Ontario, Canada
[5] Departamento de Química Física, Universidad de Valencia, 46100 Burjasot, Spain
[6] Grup Biomatemàtic de Recerca, Institut de Neurociències and Unitat de Bioestadística, Universitat Autònoma de Barcelona, 08193 Bellaterra, Spain

*Correspondence to: J. Giraldo, Grup Biomatemàtic de Recerca, Institut de Neurociències and Unitat de Bioestadística, Universitat Autònoma de Barcelona, 08193 Bellaterra, Spain.
Phone: +34 93 581 38 13
Fax: +34 93 581 23 44
E-mail: Jesus.Giraldo@uab.es

ABSTRACT

To examine the possible relationship of guanine-dependent GpA conformations with ribonucleotide cleavage, two potential of mean force (PMF) calculations were performed in aqueous solution. In the first calculation, the guanosine glycosidic (Gχ) angle was used as the reaction coordinate, and computations were performed on two GpA ionic species: protonated (neutral) or deprotonated (negatively charged) guanosine ribose $O_{2'}$. Similar energetic profiles were obtained for both ionic forms, with two minima (*anti* and *syn* Gχ). In both simulations the *anti* conformation was more stable than the *syn*, and barriers of ~4 kcal/mol for the *anti* → *syn* transition were obtained. Structural analysis showed a remarkable sensitivity of the phosphate moiety to Gχ rotation, suggesting a possible connection between Gχ orientation and the mechanism of ribonucleotide cleavage. This hypothesis was confirmed by the second PMF calculations, for which the $O_{2'}$-P distance for the deprotonated GpA was used as reaction coordinate. The computations were performed from two selected starting points: the *anti* and *syn* minima determined in the first PMF study of the deprotonated guanosine ribose $O_{2'}$. The simulations revealed that the $O_{2'}$ attack along the *syn* Gχ was more favorable than that along the *anti* Gχ: energetically, significantly lower barriers were obtained in the *syn* than in the *anti* conformation for the O-P bond formation; structurally, a lesser $O_{2'}$-P initial distance and a better suited orientation for an in-line attack was observed in the *syn* relative to the *anti* conformation. These results are consistent with the barnase-ribonucleotide catalytic interaction, for which a guanine *syn* conformation of the substrate is required to allow the abstraction of the ribose $H_{2'}$ proton by the general base Glu73, thereby suggesting a coupling between reactive substrate conformation and enzyme structure and mechanism.

INTRODUCTION

Barnase, an endoribonuclease from *Bacillus amyloliquefaciens*, catalyzes the cleavage of single-stranded RNA. The proposed catalytic mechanism[1] is that of a general acid-base, with Glu73 and His102 as the general base and general acid, respectively. The mechanism involves a trans-esterification reaction yielding a 2',3'-cyclic phosphate intermediate. This process requires the abstraction of the ribose $H_{2'}$ proton by Glu73, the formation of a covalent bond between $O_{2'}$ and the phosphorus atom, and a proton transfer from His102 to $O_{5'}$ (see Figure 1 for mechanism details and Figure 2 for the nucleotide nomenclature).[1]

Barnase cleaves ribonucleotides after guanosine either specifically or preferentially for dinucleotides and longer substrates, respectively.[2,3] Remarkably, the catalytic efficiency depends on the length of the nucleotide. It has been shown[2] that lengthening the substrate from GpX to GpXp, where X represents any nucleoside and G guanosine, produces a 10-fold decrease in K_m and a 100-fold increase in k_{cat}. Furthermore, the orientation of the guanine base relative to the ribose, governed by the guanine glycosyl torsion angle (Gχ), is key in barnase catalysis[4] (see Figure 2 for torsion angle nomenclature). The rotation of the χ angle is sterically restricted and two conformational states, *syn* and *anti*, are preferred.[5] In the *anti* conformation the base points away from the sugar moiety whereas in the *syn* conformer the base is positioned over the sugar ring. On the basis of the χ angle distribution found for mononucleoside and mononucleotide crystal structures[6] and on potential energy calculations[7] on deoxyribonucleosides, the *anti* and *syn* conformations were defined[8] as those where χ adopts values ranging between 170-300^o and 30-90^o, respectively. It has been postulated that Gχ must adopt a *syn* conformation for barnase catalysis to take place.[4] However, in the [barnase-d(CpGpApC)]$_2$ crystal structure[4] (RCSB-PDB code 1BRN), the value of

the Gχ angle is 215° (*anti* region), leading to what seems to be an unproductive conformation, where the 2'-OH, which was modeled into this structure, is pointing away (~7 Å separation) from Glu73 side chain.[4] Interestingly, modeling the bound guanosine in the *syn* conformation, followed by energy minimization of the nucleotide[4] or both the nucleotide and the enzyme,[9] positioned the 2'-OH group at a hydrogen bonding distance from Glu73 carboxylate. These derived models were shown to be consistent with the crystal structure of the complex of barnase with its natural product (3'-GMP)[10] which displays the catalytically competent *syn* Gχ conformation, allowing a Glu73–$O_{2'}$ hydrogen bond to form. Likewise, *anti* and *syn* Gχ conformations were observed in a nuclear magnetic resonance (NMR) study[11] of a barnase-3'-GMP complex in solution. In the *anti* conformation, the $O_{2'}$-H points away from Glu73, whereas in the *syn* conformation both moieties are within hydrogen bonding distance.

Nanosecond time scale molecular dynamics (MD) simulations of GpA and GpAp in water[12] and when bound to barnase,[13] were recently performed using as starting conformation the dinucleotide structure from the barnase-CGAC complex.[4] Results showed that none of the sampled conformations were in the *syn* range (0-90°). It was argued,[12,13] that the complete absence of an *anti* → *syn* transition in both GpA and GpAp during these simulations was likely due to high energy barriers that cannot be overcome at room temperature during the considered time scales. The problem of investigating the *anti*/*syn* equilibrium in oligonucleotides by MD simulations has been pointed out recently.[8] It was attributed to the requirement of surmounting conformational barriers of the type involved in the conversions between nucleic acid forms (such as B- and Z-DNA), which are not accessible during current MD time scales. This limitation does not apply to nucleosides however. MD simulations[8] of the eight (ribo- and deoxyribo-) nucleoside constituents of nucleic acids in aqueous solution were

shown to yield relatively frequent transitions between *anti* and *syn* conformations, with riboguanosine ranking second in the number of observed transitions.

The energy barrier associated with the χ angle rotation governing the *anti* to *syn* transition in both deoxyribonucleosides and deoxyribonucleotides has been recently estimated by quantum mechanical (QM) methods in vacuo.[7] In this study the malleability of this torsion angle and its dependence on the type of base and sugar stereochemistry was made evident. For each deoxyribonucleoside, four energy surfaces were obtained by varying the value of χ under γ (g^+ or *trans*) and sugar pucker (north or south) combinations. For all deoxyribonucleosides, the conformation of lowest energy was χ=*anti*, with γ=g^+ and a south (adenine, guanine, thymine) or north (cytosine) sugar pucker. The puckering mode was stable along the χ variation except for the profiles with γ = *trans* and initiated with a south sugar, where the puckering switched to the north range in the vicinity of χ=340^o or χ=50^o for all four nucleosides. High level QM calculations showed the energy barrier for the *anti* → *syn* transition to be in the range of 3.0-9.8 kcal/mol, and following the pathway through χ=120^o.[7]

In the present paper, we aim at gaining further insight into the Gχ barrier for GpA and investigate its potential relation to the catalytic mechanism of barnase. To this end, potential of mean force (PMF) calculations are carried out for this dinucleotide, in water. One series of calculations is carried out over the Gχ angle in two ionic forms of the substrate, the protonated guanosine ribose form (with $O_{2'}$-H) and the deprotonated form ($O_{2'}^-$). The second series of PMF calculations are performed over the $O_{2'}$-P distance for the deprotonated GpA form, starting from the *anti* and *syn* Gχ conformations determined for this ionic form in the first PMF calculations. The second PMF analysis aims at characterizing the energy barrier for the first step of the proposed barnase reaction mechanism, in which the deprotonated guanosine ribose $O_{2'}$ forms a

covalent bond with the phosphorus atom yielding a 2'-3'-cyclic phosphate intermediate (see above and Figures 1 and 2).

In our PMF analysis, both the 2'-OH and 3'-OH groups were included in the calculations considering the importance of the 2'-OH group in barnase catalysis and the fact that the potential energies for ribonucleotides are very sensitive to the relative orientations of these groups.[8] Our calculations furthermore included the entirety of the adenosine group in order to incorporate key effects due to the flexibility of this group and its interactions with the guanosine and phosphate moieties. Our study thus goes beyond the analysis of the intrinsic energetics of an isolated χ angle, and aims at estimating the energetics of the Gχ rotation, in both GpA and guanosine-deprotonated $O_{2'}$ GpA, in water, including and drawing especial attention to cooperative effects that the various moieties of the molecule may exert on one another.

COMPUTATONAL METHODS

Building the System

To study the behavior of GpA in aqueous solution we used the hybrid quantum mechanical and molecular mechanical (QM/MM) methodology[14-16] as implemented in the DYNAMO[17] software. This allowed us to combine the flexibility of QM methods for describing chemical reactions with the computational efficiency of MM methods. Starting configurations were taken from the crystal structure of the [barnase-d(CpGpApC)]$_2$ complex[4] (RCSB-PDB code 1BRN). The dinucleotide was solvated by adding a cubic box of 31.4 Å side dimensions, containing 995 water molecules. In each simulation, the QM subsystem comprised the dinucleotide protonated (66 atoms) or deprotonated (65 atoms) that was described by means of the semiempirical AM1 method,[18] while the water molecules were modeled using the TIP3P force field.[19] All molecular dynamics simulations were done at room temperature (300 K) and the Velocity-Verlet-Langevin algorithm was used with a time step of 1 fs. The canonical thermodynamic ensemble (NVT) was used for all calculations and periodic boundary conditions were applied. A switched outer cut-off radius of 12 Å was employed for MM-MM and QM-MM interactions.

PMF Calculations of Gχ Rotation for GpA in Water

The first goal of the present study was to evaluate the free energy barrier for the Gχ rotation in GpA in aqueous solution (see Figure 2 for atom and torsion angle notations). To this end, PMF calculations were performed taking Gχ as the reaction coordinate. To analyze whether the energy profile depends on the protonation state of the guanosine $O_{2'}$ atom, computations were performed for the protonated ($O_{2'}$-H) and deprotonated ($O_{2'}^-$) forms of the GpA molecule. In addition and importantly, the latter

calculations provided us with the structures for the study of the nucleophilic attack by the negatively charged $O_{2'}$ on the P atom, representing the step in barnase catalysis following the proton transfer from $O_{2'}$-H to Glu73 (see Figure 1).

First, 100 ps of QM/MM molecular dynamics (MD) simulations were run on the full system for both the protonated and deprotonated GpA dinucleotides. Thereafter, a minimization step was performed and a minimum (*anti* conformation) for each GpA protonation form was obtained as the starting point for the PMF calculations. The PMFs were obtained using the umbrella sampling method.[20,21] The added umbrella potential is a function of the reaction coordinate, χ (the guanosine glycosidic angle). In this study we took a harmonic form:

$$v(\chi) = \frac{1}{2} K\left(\chi - \chi^{o}\right)^{2}$$

where K is the force constant for the potential and χ^{o} is a constant reference value for the reaction coordinate. Then, a series of molecular dynamics simulations were performed with different reference values of the reaction coordinate, χ^{o} in the umbrella potential. The aim was to sample the complete range of values of χ. In practice, we found that using a force constant on the reaction coordinate of 1.5 kJ mol^{-1} rad^{-2} for the umbrella potential and reference values that differed by 0.6 degrees between simulations was sufficient to allow an adequate overlapping between consecutive simulation windows. We run 600 simulation windows for each protonated form of GpA, each consisting in 10 ps of equilibration and 10 ps of production. The values of the reaction coordinate were saved in order to obtain the histograms corresponding to each simulation, which were finally pieced together using the weighted histogram analysis method (WHAM)[22] to obtain the full probability distributions function.

PMF Calculations of Guanosine Ribose $O_{2'}$ Attack on the P Atom for GpA in Water

The second goal of the present study was to examine the relationship between the *anti* and *syn* Gχ conformations and the putative catalytic reaction mechanism (see Introduction). In particular, we investigated the second step of the enzymatic reaction, namely, the attack by the negatively charged guanosine ribose $O_{2'}$ on the P atom (see Figures 1 and 2) in the deprotonated *anti* and *syn* conformers identified in the PMF calculations described above. This involved performing PMF calculations as a function of the distance between the $O_{2'}$ and P atoms, using the same procedure described above. In these calculations, the force constant applied as constraint along the reaction coordinate was 2500 kJ mol^{-1} $Å^{-2}$. At each simulation window the reaction coordinate was increased by 0.03 Å. Starting from the *syn* conformation a total of 60 simulation windows were required to cover the whole range of interest of the reaction coordinate, while 100 simulations were needed when using the *anti* conformation as starting point. Each window consisted, as before, in 10 ps of equilibration and 10 ps of production using 1 fs time step.

Structural and Statistical Analyses

To assess representative conformations for the minima and maxima of the PMF energy profiles, the mean and standard error of the mean (SEM) of each of the dihedral angles from the set of structures (100) saved in each of the corresponding windows were calculated. When the scatter plot of any of these angles relative to Gχ (in the first PMF study) or to the guanosine $O_{2'}$-P distance (in the second PMF study) suggested the presence of more than one conformation, a K-means cluster analysis was performed. The clustering was done using the nearest centroid sorting method on the basis of

Euclidean distances computed from the nucleotide torsion angle values.[23] Since our aim was to find the minimum number of clusters able to characterize the main conformational families sampled in our systems, the number of clusters was fixed to the minimum number that was able to explain the observed angle distributions (see Ref. 12 for details). To determine which angles were responsible for the conformational differences between the initial and the final states of the PMF studies, the Student's t-test and the ANalysis Of VAriance (ANOVA) procedure, including the *post hoc* Tukey's test, were performed. *P*-values lower than 0.05 were considered statistically significant.

RESULTS

PMF for the Rotation of Gχ in solvated GpA

Figure 3 shows the PMF profiles of the Gχ torsion angle for the $O_{2'}$-H guanosine ribose (protonated) and $O_{2'}^-$ guanosine ribose (deprotonated) forms of GpA obtained in this study. Each of the profiles displays two minima and two maxima. For the protonated form, the Gχ values are -88.8°, 21.0°, 71.5°, and 140.1°, on average, for the left minimum, left maximum, right minimum, and right maximum, respectively. For the deprotonated form the corresponding values are -80.4°, 44.9°, 63.7°, and 127.4° (see Figure 3, and Tables I and II). According to a recent conformational assignment for the χ angle,[8] the two left minima correspond to *anti* conformers (170-300°) whereas the two right minima correspond to *syn* conformers (30-90°). Following the Klyne-Prelog angle notation,[5] the two left maxima are found within the +*synperiplanar* (+sp: 0° to 30°) and the +*synclinal* (+sc: 30° to 90°) regions for the protonated and deprotonated forms, respectively. The two right maxima involve guanine-ribose orientations fitting the +*anticlinal* (+ac: 90° to 150°) conformations. The latter conformations correspond to the global maxima in our simulations, indicating that the *anti* → *syn* Gχ transitions in both protonation forms of GpA would prefer a pathway through 0° rather than through 180°.

We see furthermore that both GpA ionic forms display similar energy profiles, with lower energy minima for the *anti* conformations (on the left) than for the *syn* conformations (on the right) (Figure 3). These findings are in agreement with structural data from X-ray diffraction and NMR experiments as well as with theoretical QM studies, where a preference for *anti* χ conformations was observed (see Foloppe et al.,[7] and references therein). The barriers for the *anti* → *syn* Gχ transition (through χ=0°) computed here are 4.0 and 3.9 kcal/mol for the protonated and deprotonated forms, respectively. These values are at the lower end of the range computed by QM methods

in vacuo (3.0-9.8 kcal/mol).[7] It is noteworthy that the latter analysis[7] indicated that the χ *anti* → *syn* transition occurs preferably through 120° rather than through 0° as found here. However, MD simulations in aqueous solution performed by some of the authors of the same study revealed[8] that, for purines, the *anti*/*syn* conversion takes place preferentially via $\chi = 0^{o}$, in agreement with our results. Finally, the value of ~4 kcal/mol that we compute for the *anti* → *syn* Gχ barriers is well above thermal energy at room temperature. It is therefore not too surprising that this transition was not observed in previous MD simulations.[12]

The conformational flexibility within each of the stationary states found in our Gχ PMF study was examined by plotting the fluctuation of the GpA dihedral angles (for both protonation forms) as a function of the guanosine glycosidic angle taken as the reaction coordinate (Figure 4). For most of the sampled states the measured fluctuations were indicative of a uniform conformational population. In a number of states however several conformational families could be detected. Conformations were characterized by the mean and SEM values of the dihedral angles. Depending on whether one or more conformational populations were present, these values were computed either for the full ensemble of conformations or for subgroups of the sampled conformations, derived by a k-means cluster analysis (Tables I and II for the protonated and deprotonated GpA species, respectively). Statistical analysis of the computed values indicated that most torsion angles displayed significantly different behavior in the *anti* versus *syn* conformers (see Methods), suggesting in turn that *anti* → *syn* transition is accompanied by a global conformational change of the nucleotide.

In addition we examined the conformations sampled by the *anti* and *syn* Gχ states of the deprotonated GpA for their propensity to favorably position the guanosine $O_{2'}$, the central P, and the leaving adenosine $O_{5'}$ atoms for the nucleophilic attack on the

phosphorus by the $O_{2'}$ group. Both shorter distances between $O_{2'}$ and P atoms and wider $O_{2'}$-P-$O_{5'}$ angles were found in the *syn* relative to the *anti* Gχ conformation (Figure 4B and Table II), suggesting that the ribonucleotide cleavage reaction is favored in the *syn* conformation. This is illustrated in Figure 5, which shows representatives of the *anti* and *syn* molecular structures (4.322 and 3.769 Å, for the *anti* and *syn* conformations, respectively) featuring $O_{2'}$-P distances closest to the mean values (4.32 and 3.77 Å, Table II) observed in the sampled conformations. Likewise, the corresponding $O_{2'}$-P-$O_{5'}$ angle in these structures takes the values of 81.15º and 90.10º, for the *anti* and *syn* conformers, respectively (also close to the measured mean values of 85.1º and 93.8º, Table II), and is thus more open in the *syn* than in the *anti* conformer. To further explore this hypothesis, PMF calculations along the $O_{2'}$-P distance were performed for the deprotonated GpA molecule.

PMF Calculations of the Guanosine Ribose $O_{2'}$ Attack on the P Atom in Solvated GpA

Figure 6 shows the PMF profiles of the $O_{2'}$ nucleophilic attack on the P atom for deprotonated-$O_{2'}$ GpA with the *anti* and *syn* Gχ conformations. The starting conformations were taken from the minima of the Gχ PMF profile of the deprotonated GpA form in Figure 3, and all PMF calculations were done in presence of explicit solvent. In good agreement with our first PMF calculations, the initial state for the *syn* conformation is 3.4 kcal/mol higher in energy than that of the *anti* conformation, taken as a reference. The final state is a pentacovalent intermediate with an $O_{2'}$-P covalent bond.

The most striking differences between the PMF profiles of the *syn* and *anti* GpA conformers are in the height of the energy barrier separating the initial and final states.

This barrier is 14.6 kcal/mol for the *anti* but only 2.7 kcal/mol for the *syn* conformation. These large differences likely reflect fundamental differences in the conformational and energetic landscape of the process when the latter takes place while the nucleotide adopts the *anti* or *syn* Gχ conformations (see Ref. 24 for a discussion on the stereochemistry of enzymatic reactions involving the phosphate group and a recent theoretical study on the nucleophilic attack on phosphate diesters[25]). In the following we investigate some of these differences.

Tables III and IV list the mean and SEM values of torsion angles, guanosine $O_{2'}$-P distances, and guanosine $O_{2'}$-P-adenosine $O_{5'}$ angles for the collections of 100 structures generated in each of the windows corresponding to the stationary states (the two minima and the maximum connecting both states) of the considered PMF. Our results reveal that the $O_{2'}$ attack starting from the *syn* conformation is structurally more favorable than that starting from the *anti* conformation. First, the initial distance between the two interacting atoms ($O_{2'}$ and P) is shorter for the *syn* conformation (3.55 Å versus 4.29 Å). Second, the $O_{2'}$ in the *syn* conformation is more favorably oriented for the progression of the reaction: the $O_{2'}$-P-$O_{5'}$ angle equals 130.9°, 154.6°, and 147.0° for the initial minimum, TS, and pentacovalent intermediate, respectively, whereas smaller values for this angle (84.9°, 69.2°, and 82.0) are observed for the same states in the *anti* Gχ conformation.

Comparisons between the final (pentacovalent) and the initial (either *anti* or *syn*) states of the PMF profile showed statistical significance for all the selected parameters (dihedral angles and the $O_{2'}$-P-$O_{5'}$ angle; Tables III and IV), indicating that formation of the pentacovalent species involves conformational rearrangements throughout the entire dinucleotide structure. Furthermore, the pentacovalent intermediates resulting from *anti* and *syn* Gχ conformations are structurally different as Tables III and IV show; in

particular, the dihedral angles (Gε, Gζ, Aα, and Aβ) involving the central P atom show distinct values. Figure 7 displays the representative molecular structures for the pentacovalent intermediates of the *anti* and *syn* Gχ conformational families. We see that within the *syn* Gχ conformation, the attacking $O_{2'}$ and leaving $O_{5'}$ groups are situated approximately at the apical positions of a trigonal bipyramid, thereby fitting an in-line mechanism for ribonucleotide cleavage. In contrast, the attack from the *anti* Gχ conformation resembles an adjacent mechanism, for which the nucleophile enters on the same side as the leaving group. It is worth noting that the *syn* minimum obtained in the PMF and described in Table IV is different from that reported in Table II obtained from the conformational PMF. In particular, the values of the $O_{2'}$-P distance and the $O_{2'}$-P-$O_{5'}$ angle show that the present *syn* minimum is slightly more advanced for the nucleophilic attack on the phosphorus atom. This difference is not unexpected as the conformational and reaction PMFs are obtained using different reaction coordinates, corresponding to the integration over different regions of the configurational space. In addition, the behavior of the PMF presented in Figure 6 shows that the free energy landscape can be quite flat for large $O_{2'}$-P distances in the *syn* conformation and thus no important free energy differences are expected between the two reported (Tables II and IV) *syn* minima.

Taken together, the energy differences between the *anti* and *syn* minima of deprotonated-$O_{2'}$ GpA and the barriers for both the Gχ rotation and the $O_{2'}$ attack on the phosphorus atom in both the *anti* or *syn* conformations (Figures 3 and 6) lead us to postulate that the nucleophilic attack on the phosphorus atom by the $O_{2'}$ takes place when the GpA molecule adopts the syn conformation. With our analysis confirming that the *anti* conformation of the dinucleotide is the predominant molecular species in solution, and hence likely to be that of the substrate of the enzymatic reaction, we

conclude that an *anti* → *syn* transition of the glycosidic angle must occur prior to the nucleophilic attack.

DISCUSSION AND CONCLUDING REMARKS

The general acid-base mechanism[1] proposed for barnase catalysis, with Glu73 acting as the general base, together with structural data from nucleotide-barnase complexes[4,9-11] suggest that a *syn* conformation for the Gχ angle is required in order to allow the abstraction of the ribose $H_{2'}$ proton by Glu73, a key step of barnase catalysis. The work described here provides insight into the link between this requirement and the intrinsic conformational properties of the solvated nucleotide and, by the same token, allows us to gauge the role that the enzyme scaffold may play. The first PMF calculations for GpA in water as a function of the Gχ torsion angle allowed us to characterize the influence of this angle on the GpA conformational landscape. In addition it also provided us with the initial structures for studying the nucleophilic attack by the ribose $O_{2'}$ on the P atom. Our second series of calculations, which simulated the $O_{2'}$-P covalent bond formation, showed that the *syn* Gχ conformation favors the in-line attack of the nucleophile. Since the nucleophile is believed to be produced through proton abstraction by the catalytic residue Glu73, our latter finding thus provide a rationalization for the relative orientation of this residue in the barnase active site.

It is noteworthy to relate the conclusions from our PMF calculations in water with information derived from the crystal structure of the barnase-d(CGAC)] complex,[4] where the guanine base adopts an *anti* conformation, and from a modeled barnase-5'3'(AAGAAp)-O-methyl ester complex,[9] in which Gχ was rotated to achieve a *syn* conformation. In the crystal structure, the guanosine $O_{2'}$ atom, which was added to the coordinates of the bound deoxynucleotide, was found to be positioned ~7 Å away from the carboxylate of Glu73, too far to enable proton abstraction by the latter. On the other hand, in the modeled complex,[9] the corresponding groups were positioned at a hydrogen

bonding distance, optimal for proton abstraction (Figure 8). What more, in both the crystal and modeled complexes, the GpA molecule displays conformational properties in good agreement with those described in this work. Thus, for the *syn* guanosine (Figure 8 right), the $O_{2'}$ (following proton abstraction by Glu73) is correctly oriented towards the P-$O_{5'}$ bond for an in-line attack. This is clearly not the case for the guanosine in the *anti* conformation (Figure 8 left). It is thus quite remarkable to see that two seemingly distinct processes, the initiation of catalysis through the abstraction of the $O_{2'}$ proton and the conformational transitions towards the pentacovalent intermediate, are both fostered by the Gχ *syn* conformation of the nucleotide and not the *anti* state.

The work presented here, and in particular the results on the lower energy barrier for reaching the pentacovalent intermediate in the *syn* versus the anti conformation clearly concern only the solvated unbound GpA molecule. They hence provide no information on the GpA conformer (*syn* or *anti*) that may bind to the enzyme active site, or in the case that the *anti* conformation is the one to bind, what the barrier for the *anti* to *syn* transition might be for the bound dinucleotide. It should be mentioned however, that the only known case of GpA bound to barnase adopting the Gχ *anti* conformation is that of the [barnase-d(CGAC)] crystal structure,[4] where the ligand is a deoxynucleotide inhibitor that cannot be cleaved by the enzyme.

Overall therefore, our calculations and the above considerations suggest that there exists a link between Gχ torsion angle adopting a *syn* conformation and the requirement to have a negatively charged $O_{2'}$ in order to carry out the in-line attack on the phosphorus atom. This in turn suggests that the active site of barnase might have been shaped by evolution in a way in which abstraction of $H_{2'}$ and in-line orientation of $O_{2'}$ were coupled. This idea is in agreement with the concept of enzyme

preorganization.[26] According to this concept, the catalytic power of an enzyme is mainly due to transition state stabilization (TSS), achieved through the electrostatic environment provided by its active site. The greater similarity between the transition state (TS) and the catalytic conformation than between the TS and the noncatalytic conformations[27,28] suggests that TSS involves the destabilization of the noncatalytic conformations (*anti* Gχ conformation in barnase catalysis), thereby providing an additional rate enhancement of the enzyme catalyzed reaction relative to its uncatalyzed counterpart in solution.[29]

Coupling between a specific substrate conformation and molecular reactivity and the connection of this property with enzyme structure and mechanism may illustrate the functioning of enzymes as finest machines, evolved to optimize all the processes that favor the productive pathway of the reactions they catalyze. To explore further these ideas, studies of the ribonucleotide cleavage in the barnase environment are in progress.

ACKNOWLEDGEMENTS

V.M. thanks the DGI for projects DGI CTQ2006-15447-C02-01/BQU, UJI-BANCAIXA foundation for project P1·1B2005-13 and Generalitat Valenciana for project GV06/152. I.T. is indebted to Ministerio Educación y Ciencia for project CTQ2006-15447-CO2-02 and Generalitat Valenciana for project GV06-021. J.G. is grateful to Ministerio de Educación y Ciencia for project SAF2004-06134.

References

1. Mossakowska DE, Nyberg K, Fersht AR. Kinetic characterization of the recombinant ribonuclease from Bacillus amyloliquefaciens (barnase) and investigation of key residues in catalysis by site-directed mutagenesis. Biochemistry 1989;28:3843-3850.

2. Day AG, Parsonage D, Ebel S, Brown T, Fersht AR. Barnase has subsites that give rise to large rate enhancements. Biochemistry 1992;31:6390-6395.

3. Rushizky GW, Greco AE, Hartley RW, Sober HA. Studies on B. subtilis Ribonuclease. I. Characterization of Enzymatic Specificity. Biochemistry 1963;2:787-793.

4. Buckle AM, Fersht AR. Subsite binding in an RNase: structure of a barnase-tetranucleotide complex at 1.76-Å resolution. Biochemistry 1994;33:1644-1653.

5. Saenger W. Principles of nucleic acid structure. New York: Springer-Verlag; 1988.

6. Gelbin A, Schneider B, Clowney L, Hsieh S-H, Olson WK, Berman HM. Geometric parameters in nucleic acids: sugar and phosphates constituents. J Am Chem Soc 1996;118:519-529.

7. Foloppe N, Hartmann B, Nilsson L, MacKerell AD, Jr. Intrinsic conformational energetics associated with the glycosyl torsion in DNA: a quantum mechanical study. Biophys J 2002;82:1554-1569.

8. Foloppe N, Nilsson I. Toward a full characterization of nucleic acid components in aqueous solution: simulations of nucleosides. J Phys Chem B 2005;109:9119-9131.

9. Gordon-Beresford RM, Van Belle D, Giraldo J, Wodak SJ. Effect of nucleotide substrate binding on the pKa of catalytic residues in barnase. Proteins 1996;25:180-194.

10. Guillet V, Lapthorn A, Mauguen Y. Three-dimensional structure of a barnase-3'GMP complex at 2.2 Å resolution. FEBS Lett 1993;330:137-140.

11. Meiering EM, Bycroft M, Lubienski MJ, Fersht AR. Structure and dynamics of barnase complexed with 3'-GMP studied by NMR spectroscopy. Biochemistry 1993;32:10975-10987.

12. Giraldo J, Wodak SJ, Van Belle D. Conformational analysis of GpA and GpAp in aqueous solution by molecular dynamics and statistical methods. J Mol Biol 1998;283:863-882.

13. Giraldo J, De Maria L, Wodak SJ. Shift in nucleotide conformational equilibrium contributes to increased rate of catalysis of GpAp versus GpA in barnase. Proteins 2004;56:261-276.

14. Warshel A, Levitt M. Theoretical studies of enzymic reactions: dielectric, electrostatic and steric stabilization of the carbonium ion in the reaction of lysozyme. J Mol Biol 1976;103:227-249.

15. Gao J, Truhlar DG. Quantum mechanical methods for enzyme kinetics. Annu Rev Phys Chem 2002;53:467-505.

16. Martí S, Roca M, Andrés J, Moliner V, Silla E, Tuñón I, Bertrán J. Theoretical insights in enzyme catalysis. Chem Soc Rev 2004;33:98-107.

17. Field MJ, Albe M, Bret C, Proust-De Martin F, Thomas A. The dynamo library for molecular simulations using hybrid quantum mechanical and molecular mechanical potentials. J Comp Chem 2000;21:1088-1100.

18. Dewar MJS, Zoebisch EG, Healey EF, Stewart JJP. AM1: A new general purpose quantum mechanical molecular model. J Am Chem Soc 1985;107:3902-3909.

19. Jorgensen WL, Chandrasekhar J, Madura JF, Impey RW, Klein ML. Comparison of simple potential functions for simulating liquid water. J Chem Phys 1983;79:926-935.

20. Valleau JP, Torrie GM. A guide to Monte Carlo for statistical mechanics: Byways. In: Statistical mechanics A. Modern theoretical chemistry New York: Berne B J (ed): Plenum Press; 1977**.** p 169-194.

21. Torrie GM, Valleau JP. Nonphysical sampling distributions in Monte Carlo free energy estimation: Umbrella sampling. J Comp Phys 1977;23:187-199.

22. Kumar S, Bouzida D, Swendsen RH, Kollman PA, Rosenberg JM. The weighted histogram analysis method for free energy calculations on biomolecules. I. The method. J Comp Chem 1992;13:1021.

23. Afifi AA, Clark V. Cluster analysis. In: Computer-aided multivariate analysis London: Chapman & Hall; 1996**.** p 381-409.

24. Fersht AR. Stereochemistry of enzymatic reactions. In: Structure and mechanism in protein science. A guide to enzyme catalysis and protein folding New York: W. H. Freeman and Company; 1999**.** p 245-272.

25. López X, Dejaegere A, Leclerc F, York DM, Karplus M. Nucleophilic attack on phosphate diesters: a density functional study of in-line reactivity in dianionic, monoanionic, and neutral systems. J Phys Chem B Condens Matter Mater Surf Interfaces Biophys 2006;110:11525-11539.

26. Warshel A. Electrostatic origin of the catalytic power of enzymes and the role of preorganized active sites. J Biol Chem 1998;273:27035-27038.

27. Martí S, Andrés J, Moliner V, Silla E, Tuñón I, Bertrán J. A Comparative Study of Claisen and Cope Rearrangements Catalyzed by Chorismate Mutase. An Insight into Enzymatic Efficiency: Transition State Stabilization or Substrate Preorganization? J Am Chem Soc 2004;126:311-319.

28. Martí S, Andrés J, Moliner V, Silla E, Tuñón I, Bertrán J. Preorganization and reorganization as related factors in enzyme catalysis: the chorismate mutase case. Chem Eur J 2003;9:984-991.

29. Giraldo J, Roche D, Rovira X, Serra J. The catalytic power of enzymes: conformational selection or transition state stabilization? FEBS Lett 2006;580:2170-2177.

Figure legends

Figure 1. Schematic representation of the first two steps of ribonucleotide cleavage mechanism by barnase. Step 1: Glu73 picks up a proton from ribose $O_{2'}$ (see Figure 2 for atom notation) and the negatively charged $O_{2'}$ attacks on and makes a covalent bond with the P atom. Step 2: The positively charged His102 gives a proton to $O_{5'}$ and the $O_{5'}$-P bond breaks.

Figure 2. Notation scheme for atoms and torsion angles in GpA. Torsion angles are defined as: α=$O_{3'}$-P-$O_{5'}$-$C_{5'}$, β=P-$O_{5'}$-$C_{5'}$-$C_{4'}$, γ=$O_{5'}$-$C_{5'}$-$C_{4'}$-$C_{3'}$, δ=$C_{5'}$-$C_{4'}$-$C_{3'}$-$O_{3'}$, ε=$C_{4'}$-$C_{3'}$-$O_{3'}$-P, ζ=$C_{3'}$-$O_{3'}$-P-$O_{5'}$, χ=$O_{4'}$-$C_{1'}$-N_9-C_4. For a given X angle, GX and AX stand for guanosine and adenosine X angles, respectively.

Figure 3. PMF profiles of the Gχ rotation for two GpA ionic forms in water: protonated (guanosine ribose $O_{2'}$-H) GpA (green line) and deprotonated (guanosine ribose $O_{2'}^-$) GpA (red line).

Figure 4. Scatter plots of Gχ with the rest of dihedral angles for the stationary states (minima and maxima) found in Figure 3. A) Protonated GpA. B) Deprotonated GpA. For the Gχ, the (-180^o to $+180^o$) range was chosen; for the other angles, the former or the (0^o to 360^o) ranges were selected; nevertheless, the polar nature of angles should be taken into account when looking at the plots. In Figure B (deprotonated GpA), the guanosine $O_{2'}$-P distance and the guanosine $O_{2'}$-P-adenosine $O_{5'}$ angle are also examined.

Figure 5. Molecular structures of deprotonated GpA representative members of the *anti* and *syn* stationary states obtained in the PMF profile of the Gχ rotation displayed in Figure 3. These structures have been selected because they are those with the guanosine $O_{2'}$-P distances closest to their corresponding conformational group mean values (Table II). The *syn* conformation favors the $O_{2'}$ attack on the P atom relative to the *anti* conformation: $O_{2'}$-P distances of 3.769 and 4.322 Å and $O_{2'}$-P-$O_{5'}$ angles of 90.10º and 81.15º for the *syn* and *anti* conformations, respectively. The guanosine ribose $O_{2'}$ and the P atoms are connected by a dotted line.

Figure 6. PMF profiles (red: *anti* Gχ and green: *syn* Gχ) of the $O_{2'}$ attack on the P atom for deprotonated (guanosine ribose $O_{2'}^-$) GpA. The *anti* and *syn* Gχ starting points were taken from previously determined minima (Figure 3): the *syn* is higher in energy than the *anti*, being the latter taken as the reference (0 kcal/mol).

Figure 7. Molecular structures representative of the pentacovalent intermediates obtained in the PMF profiles of the $O_{2'}$ attack displayed in Figure 6 from either *anti* or *syn* Gχ conformations. The structure for the Gχ *syn* conformation (on the right), in contrast to the structure for the *anti* Gχ conformation (on the left), displays a trigonal bipyramid with the entering and leaving groups in apical positions.

Figure 8. Molecular structures showing the conformational arrangement of the GpA fragment for barnase-d(CGAC) crystal[4] (left) and barnase-5'3'(AAGAAp)-*O*-methyl ester modeled[9] (right) complexes. For the crystal structure the ribose $O_{2'}$ atoms were modeled because deoxyribonucleotides need to be used in experimental studies to avoid enzyme catalysis. In the crystal complex the guanosine displays an *anti* conformation

(Gχ=215^{o}) whereas in the modeled complex the guanosine displays a *syn* conformation (Gχ=95^{o}). In the *anti* conformation, the guanosine $O_{2'}$ is far away (~7 Å) from the oxygens of Glu73 whereas in the *syn* conformation, a hydrogen bonding distance between both moieties is found. In the *syn* guanosine conformation the $O_{2'}$ is correctly positioned for an in-line attack on the P atom (once its proton is abstracted by Glu73) in contrast to the *anti* guanosine conformation.

TABLE I. Gχ PMF study: Torsion and pseudorotation angles for protonated ($O_{2'}$-H) GpA.

Torsion and pseudorotation angles	Minimum (*anti*)	TS (*anti* → *syn*)	Minimum (*syn*)	Absolute maximum
Gχ	-88.8± 0.1	21.0±0.1	71.5±0.1	140.1±0.1
Gγ	192.1±0.9*	295.9±1.1	277.9±0.9	167.2±1.4
Gδ	141.6±0.7	127.0±0.6	140.0±0.6	126.3±0.6
Gp	194.1±2.2	N=10 83.8±13.9 N=90 246.1±3.2	188.9±1.8	290.6±3-1
Gε	237.2±0.7*	279.6±0.8	277.6±0.8	202.2±1.0
Gζ	215.4±1.0*	176.8±0.6	116.9±1.2	108.8±1.3
Aχ	82.4±1.0*	59.6±0.9	88.9±1.3	63.8±1.1
Aα	98.8±1.0*	297.3±1.0	153.3±2.6	182.3±2.0
Aβ	73.4±1.2*	173.8±1.0	156.9±2.1	155.0±1.3
Aγ	181.1±0.8*	188.5±0.8	279.3±1.8	193.8±1.5
Aδ	125.4±0.7	119.7±0.7	124.6±0.5	100.8±0.7
Ap	N=38 213.1±6.5^{A,B} N=62 121.5±3.6^{B}	115.8±2.2	A N=88 281.6±3.2 B N=12 114.0±13.9	N=7 327.5±7.1 N=93 45.3±2.3

Mean ± standard errors of torsion angles of 100 structures saved in each of the windows corresponding to the stationary states of Gχ PMF energy profile (Figure 3). A K-means cluster analysis was used when scatter plots (Fig. 4A) suggested that more than one conformational family was present. Gp and Ap correspond to the pseudorotation angles for guanosine and adenosine riboses, respectively. Comparisons between *anti* and *syn* conformations for each of the angles were performed by Student's t-test or the Tukey's *post hoc* test if two or more than two conformational populations were involved, respectively. *P*-values lower than 0.05 are indicated by * and considered statistically significant. If the *syn* conformation presents two subpopulations (A,B) then A and/or B in the *anti* conformation indicates statistical significance with A and/or B *syn* conformation, respectively.

TABLE II. Gχ PMF study: Torsion and pseudorotation angles, guanosine $O_{2'}$-P distance, and guanosine $O_{2'}$-P-$O_{5'}$ adenosine angle for deprotonated ($O_{2'}^-$) GpA.

Variables	Minimum (*anti*)	TS (*anti* → *syn*)	Minimum (*syn*)	Absolute maximum
Gχ	-80.4±0.1	44.9±01	63.7±0.1	127.4±0.1
Gγ	46.6±1.2*	173.2±0.8	182.4±1.7	178.2±1.1
Gδ	143.8±0.6*	141.7±0.6	136.8±0.7	125.2±0.6
Gp	204.9±1.5*	195.7±1.3	187.8±2.2	277.5±1.8
Gε	291.0±1.0*	246.3±1.0	232.1±0.8	240.5±1.0
Gζ	197.5±1.6	209.0±1.4	194.4±0.8	178.7±0.9
Aχ	150.9±1.1*	262.3±0.9	260.9±0.8	276.1±0.8
Aα	N=44 220.3±2.3* N=56 121.1±2.5*	143.1±1.2	143.2±1.2	70.3±1.2
Aβ	N=23 63.0±1.5* N=33 28.1±3.9* N=44 76.3±2.5*	89.7±1.6	100.5±1.0	105.4±0.9
Aγ	169.5±3.1*	178.7±0.9	177.6±0.9	194.2±0.8
Aδ	120.5±0.8	126.0±0.8	122.6±0.8	138.5±0.9
Ap	N=23 308.5±3.7^{A,B} N=69 262.9±2.2^{B} N=3 81.2±7.3^{A,B} N=5 12.0±3.0^{A}	N=20 277.7±6.5 N=72 196.5 ±3.6 N=8 64.5 ±11.6	A N=92 263.8±3.5 B N=8 23.3± 6.3	241.1±2.6
Guanosine $O_{2'}$-P distance	4.32±0.01*	3.96±0.01	3.77±0.01	3.97±0.02
Guanosine $O_{2'}$-P- adenosine $O_{5'}$ angle	85.1±0.5*	85.6±0.8	93.8±0.6	98.7±0.4

Mean ± standard errors of torsion angles, guanosine $O_{2'}$-P distances, and guanosine $O_{2'}$-P-$O_{5'}$ adenosine angles of 100 structures saved in each of the windows corresponding to the stationary states of Gχ PMF energy profile (Figure 3). A K-means cluster analysis was used when scatter plots (Fig. 4B) suggested that more than one conformational family was present. Gp and Ap correspond to the pseudorotation angles for guanosine and adenosine riboses, respectively. Comparisons between *anti* and *syn* conformations for each of the variables were performed by Student's t-test or Tukey's *post hoc* test if two or more than two populations were involved, respectively. *P*-values lower than 0.05 are indicated by * and considered statistically significant. If the *syn* conformation presents two subpopulations (A,B) then A and/or B in the *anti* conformation indicates statistical significance with A and/or B *syn* conformation, respectively.

TABLE III. Guanosine $O_{2'}$→P PMF study under *anti* Gχ conformation: Torsion and pseudorotation angles, guanosine $O_{2'}$-P distance, and guanosine $O_{2'}$-P-adenosine $O_{5'}$ angle for deprotonated ($O_{2'}^-$) GpA.

Variables	Minimum (*anti*)	TS (*anti*→pentacovalent)	Minimum (pentacovalent from *anti*)
Gχ	-64.3±0.7*	-59.1±0.8	-72.6±0.9
Gγ	81.7±1.5*	68.8±1.6	67.2±1.2
Gδ	140.1±0.6*	135.6±0.8	115.5±0.7
Gp	212.0±2.0*	217.5±2.8	-2.6±7.5
Gε	289.0±0.9*	181.7±0.9	106.2±0.7
Gζ	181.3±1.0*	268.7±1.3	-8.7±2.2
Aχ	182.9±0.8*	168.5±1.1	189.2±1.0
Aα	111.5±0.9*	243.1±0.8	124.8±2.0
Aβ	58.5±1.2*	288.2±0.9	66.2±2.0
Aγ	151.0±*	233.9±0.6	142.1±1.5
Aδ	144.4±0.9*	147.8±0.9	126.2±1.4
Ap	227.6±1.2*	240.0±1.5	-82.7±4.6
Guanosine $O_{2'}$-P distance	4.29±0.00	2.78±0.00	1.74±0.00
Guanosine $O_{2'}$-P-$O_{5'}$ adenosine angle	84.9±0.4*	69.2±0.4	82.0±0.3

Mean ± standard errors of torsion angles, guanosine $O_{2'}$-P distances, and guanosine $O_{2'}$-P- adenosine $O_{5'}$ angles of 100 structures saved in each of the windows corresponding to the stationary states of the guanosine $O_{2'}$ attack on the P atom from a PMF energy profile (Figure 6). Gp and Ap correspond to the pseudorotation angles for guanosine and adenosine riboses, respectively. Comparisons between Minimum *anti* and Minimum pentacovalent conformations for each of the variables were performed by Student's t-test. *P*-values lower than 0.05 are indicated by * and considered statistically significant.

TABLE IV. Guanosine $O_{2'}$→P PMF study under *syn* Gχ conformation: Torsion and pseudorotation angles, guanosine $O_{2'}$-P distance, and guanosine $O_{2'}$-P-adenosine $O_{5'}$ angle for deprotonated ($O_{2'}^-$) GpA.

Variables	Minimum (*syn*)	TS (*syn*→pentacovalent)	Minimum (pentacovalent from *syn*)
Gχ	71.0±0.9*	96.5±1.0	74.9±0.9
Gγ	38.2±2.4*	59.1±2.8	47.8±1.9
Gδ	124.2±0.6*	141.4±0.6	121.9±0.9
Gp	155.0±3.0*	184.1±2.0	125.4±3.0
Gε	219.2±0.6*	183.4±0.6	139.0±1.5
Gζ	144.8±0.8*	136.4±0.8	180.2±1.7
Aχ	83.3±1.5*	78.3±1.4	77.2±0.8
Aα	108.4±1.1*	113.4±1.1	144.1±2.0
Aβ	144.4±1.1*	146.6±1.0	153.6±1.3
Aγ	177.7±0.8*	189.1±0.9	189.6±0.9
Aδ	110.0±1.0*	109.2±0.8	113.2±0.8
Ap	18.0±5.0*	-23.9±3.9	-26.6±5.1
Guanosine $O_{2'}$-P distance	3.55±0.00	2.69±0.00	1.80±0.00
Guanosine $O_{2'}$-P-$O_{5'}$ adenosine angle	130.9±0.4*	154.6±0.4	147.0±1.1

Mean ± standard errors of torsion angles, guanosine $O_{2'}$-P distances, and guanosine $O_{2'}$-P-$O_{5'}$ adenosine angles of 100 structures saved in each of the windows corresponding to the stationary states of the guanosine $O_{2'}$ attack on the P atom from a PMF energy profile (Figure 6). Gp and Ap correspond to the pseudorotation angles for guanosine and adenosine riboses, respectively. Comparisons between Minimum *anti* and Minimum pentacovalent conformations for each of the variables were performed by Student's t-test. *P*-values lower than 0.05 are indicated by * and considered statistically significant.

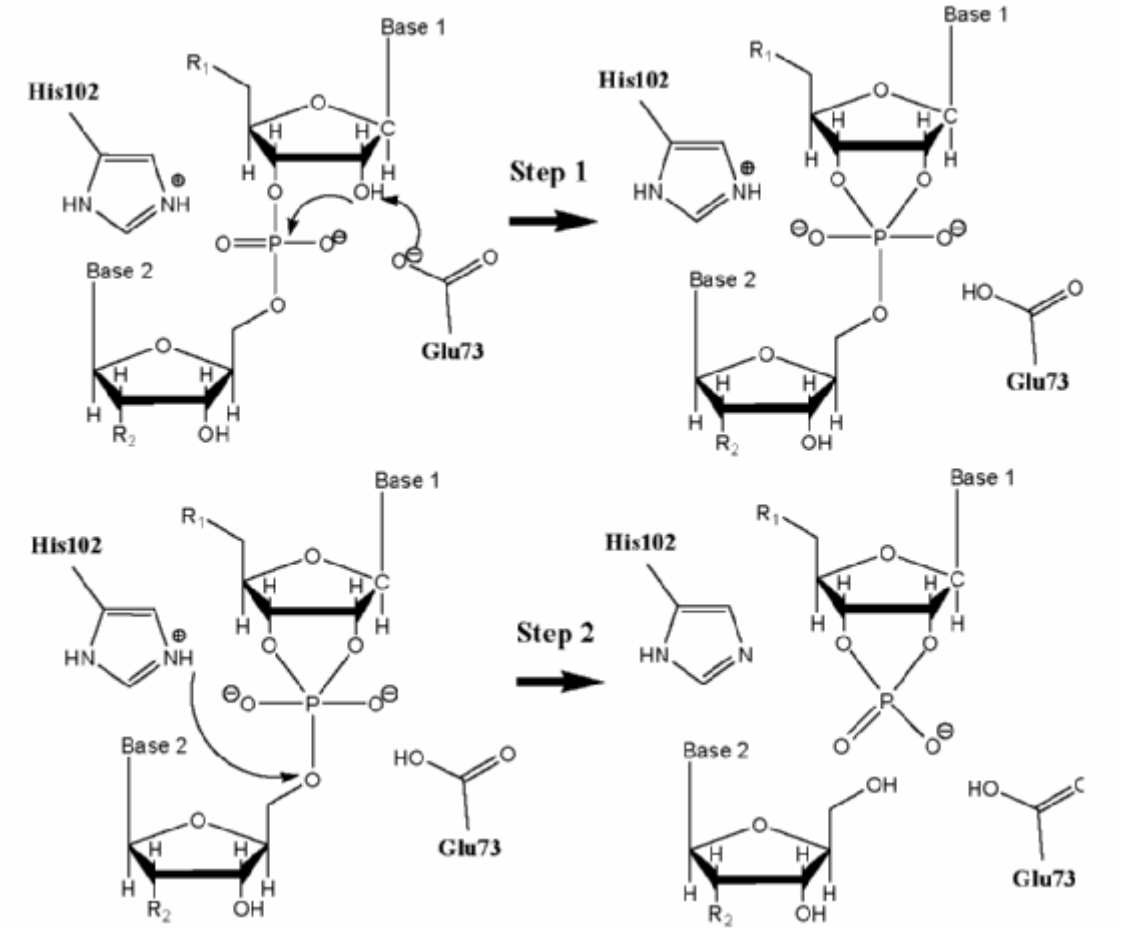

Fig. 1

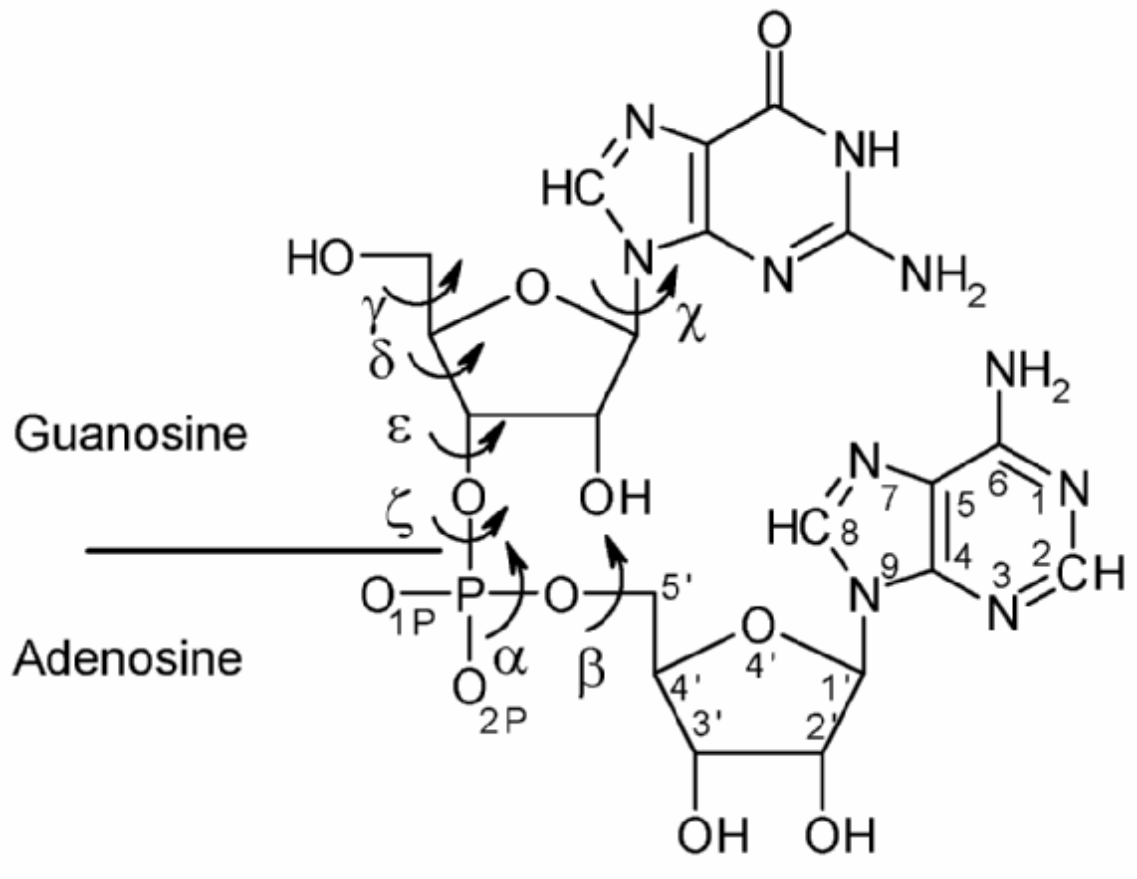
Guanosine
Adenosine
HO
O
N
NH
HC
N
N
NH2
γ
δ
ε
ζ
χ
O
OH
O1P
P
O
O2P
α
β
5'
4'
1'
3'
2'
OH
OH
NH2
N
HC
N
N
CH
1
2
3
4
5
6
7
8
9

Fig. 2

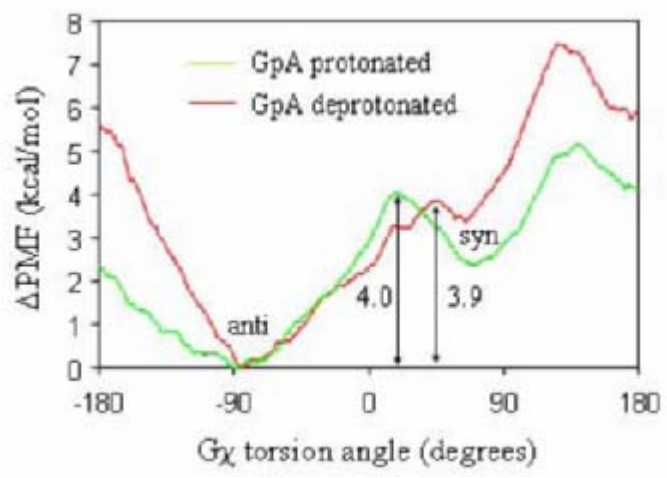
GpA protonated
GpA deprotonated
ΔPMF (kcal/mol)
anti
syn
4.0
3.9
Gχ torsion angle (degrees)

Fig. 3

a

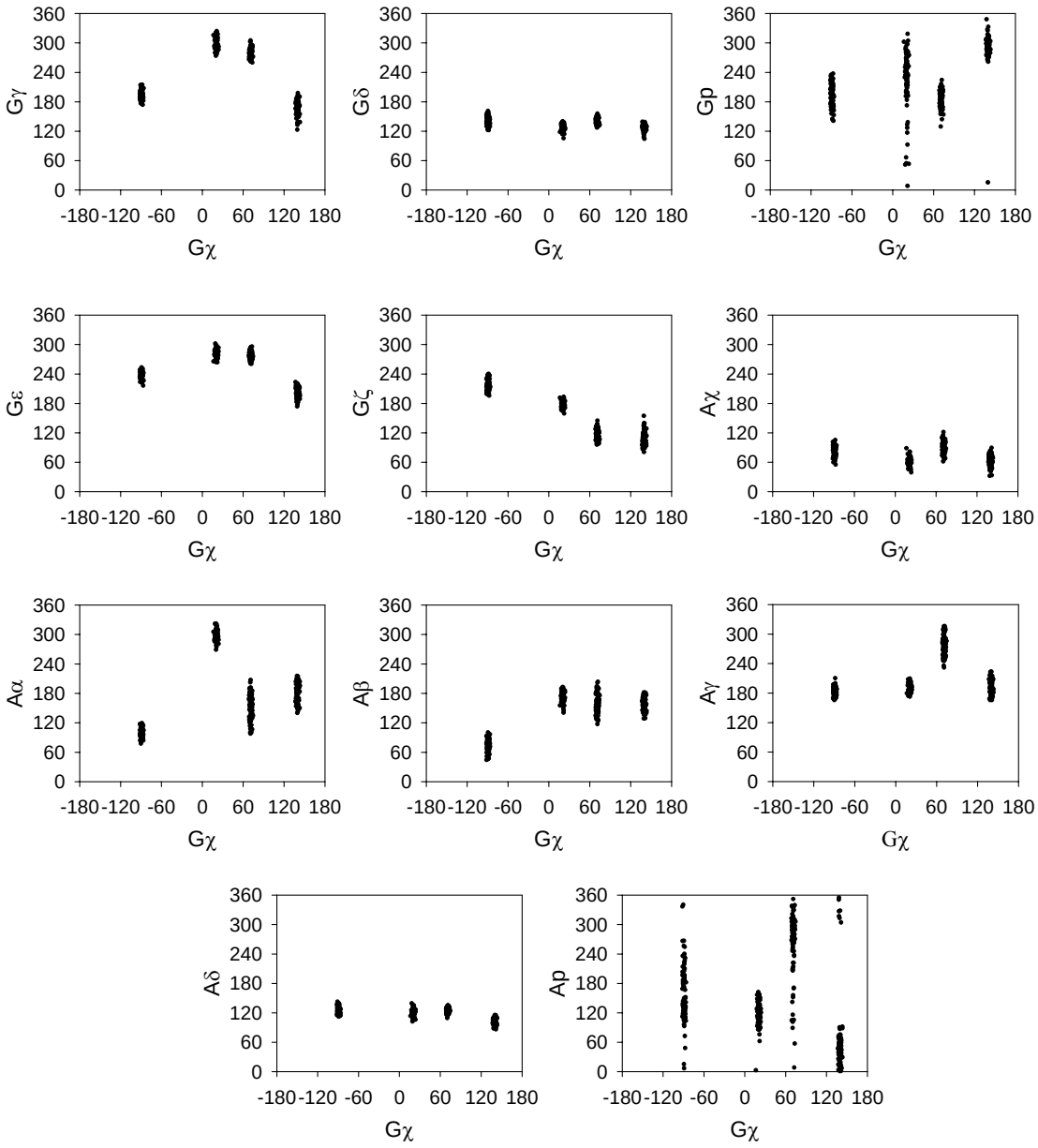
Gγ
Gδ
Gp
Gε
Gζ
Aχ
Aα
Aβ
Aγ
Aδ
Ap
Gχ
360
300
240
180
120
60
0
-180 -120 -60 0 60 120 180

Fig. 4

b

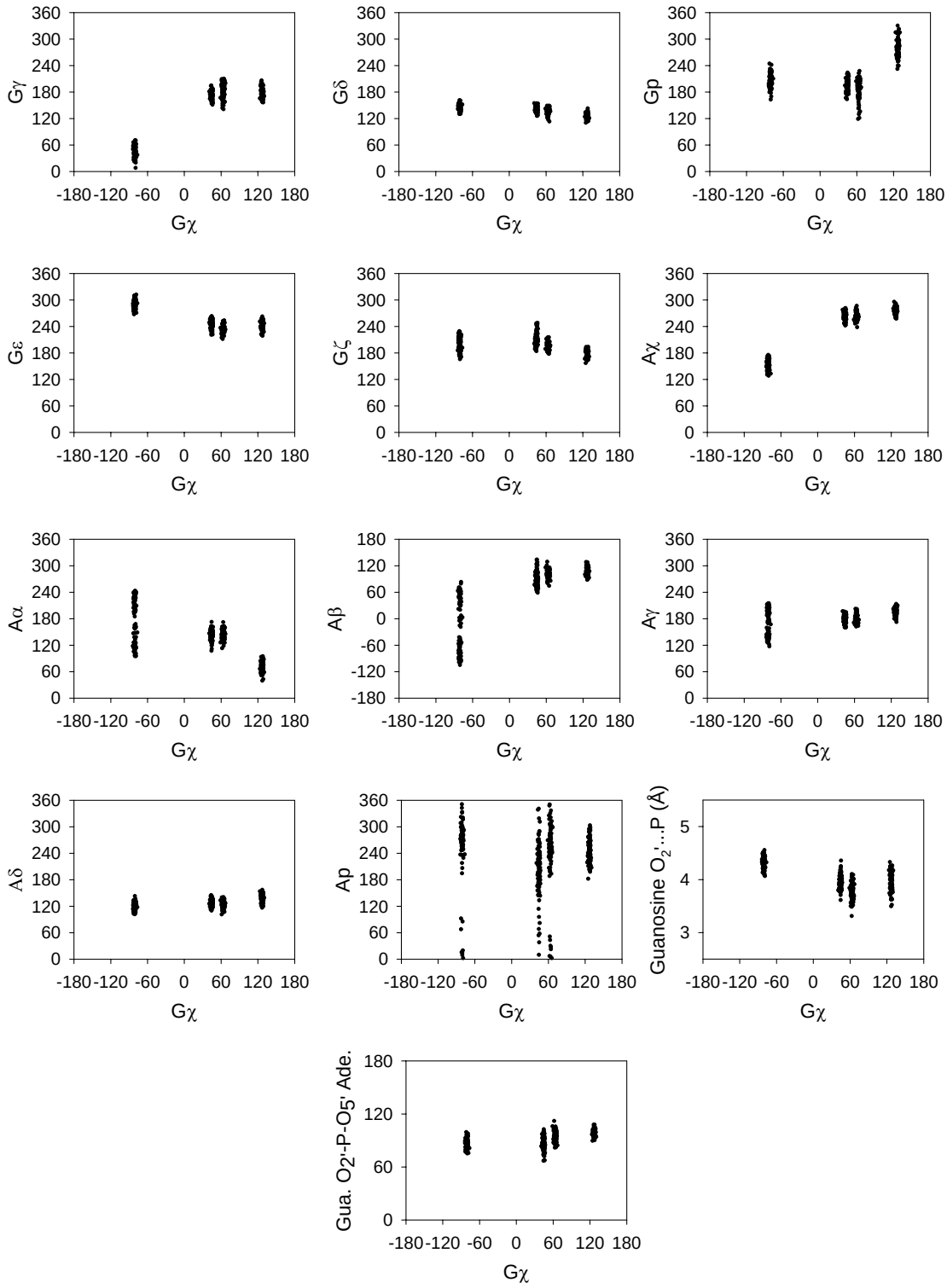
Gγ
Gδ
Gp
Gε
Gζ
Aχ
Aα
Aβ
Aγ
Aδ
Ap
Guanosine O2'...P (Å)
Gua. O2'-P-O5' Ade.
Gχ
-180 -120 -60 0 60 120 180
0 60 120 180 240 300 360
-180 -120 -60 0 60 120 180
3 4 5

Fig. 4

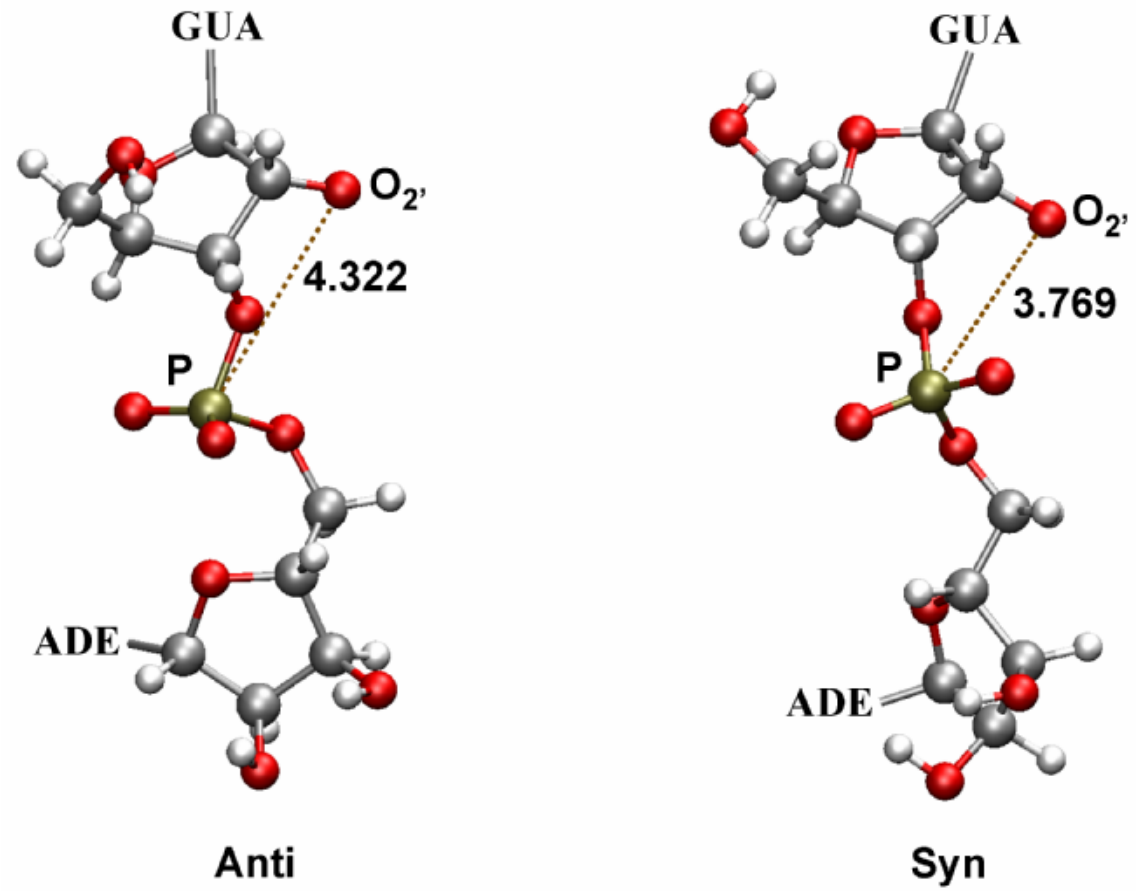

Fig. 5

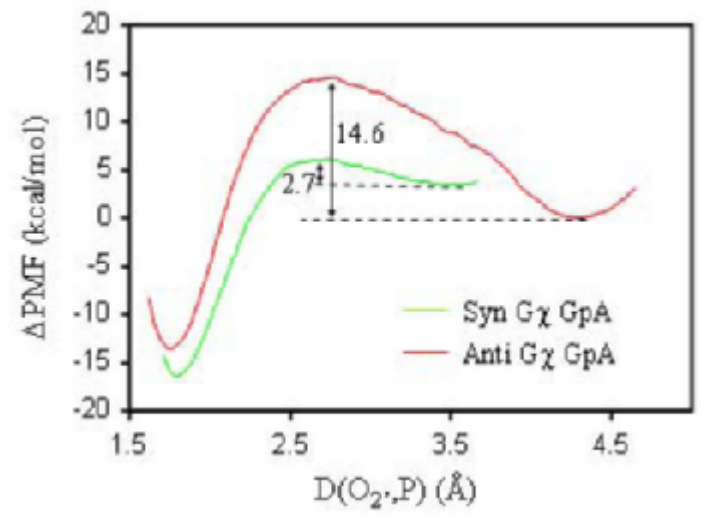
20
15
10
5
0
-5
-10
-15
-20
ΔPMF (kcal/mol)
14.6
2.7
Syn Gχ GpA
Anti Gχ GpA
1.5
2.5
3.5
4.5
D(O2',P) (Å)

Fig. 6

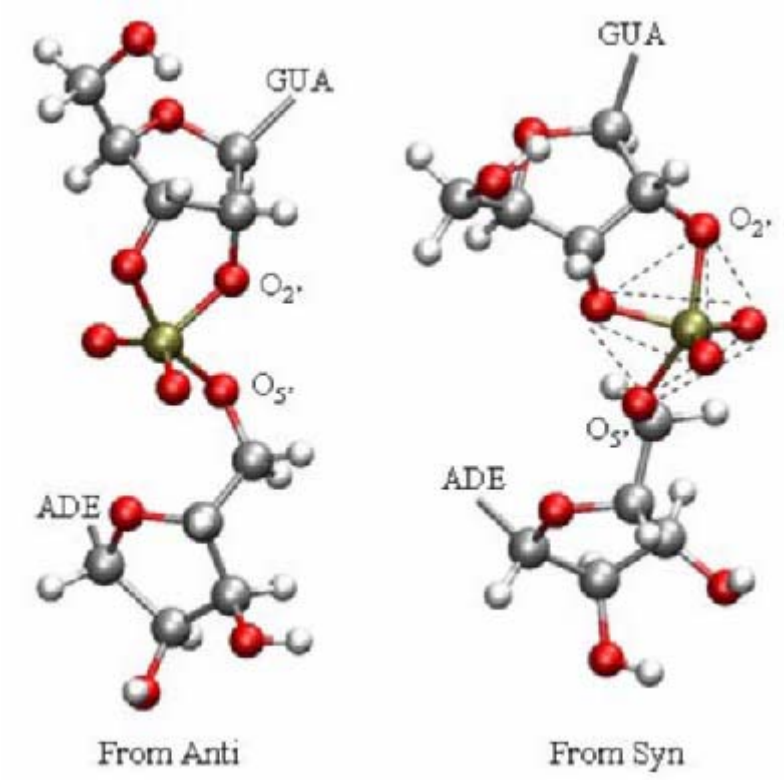

Fig. 7

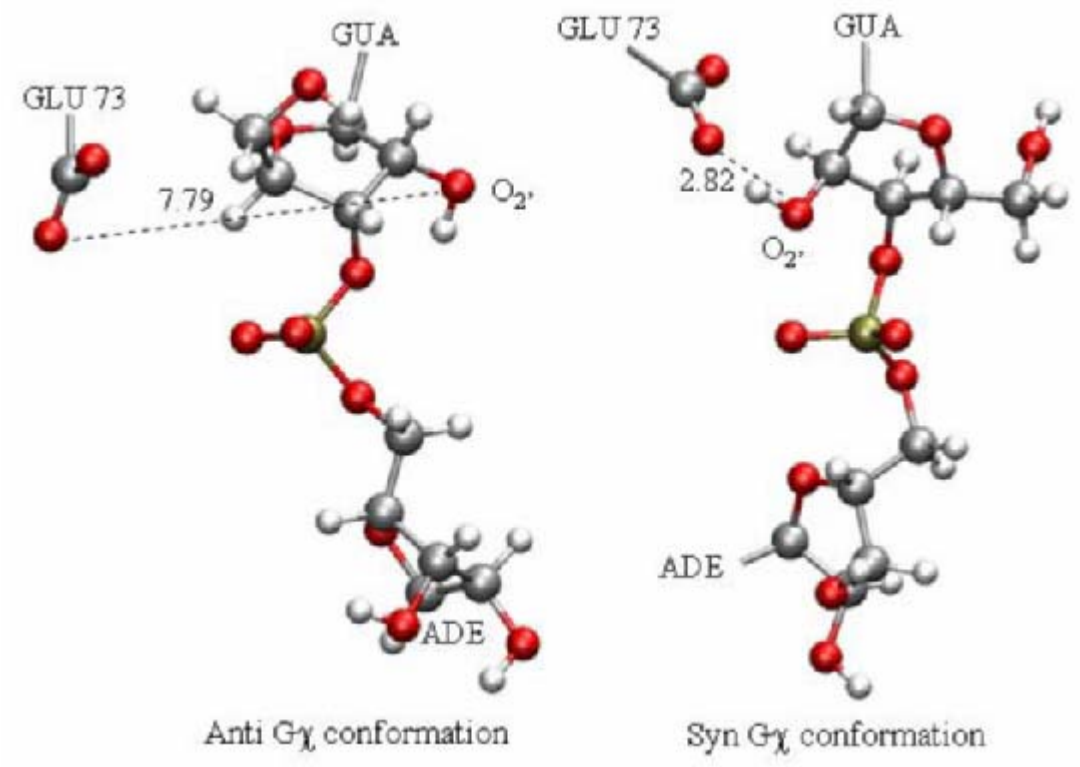
GUA
GLU 73
7.79
O2'
ADE
Anti Gχ conformation
GLU 73
GUA
2.82
O2'
ADE
Syn Gχ conformation

Fig. 8